ORIGINAL PAPER

Thin films of Pd and Pd–1% MWCNT as new electrocatalysts for oxidation of phenol in acid medium

Ravindra Nath Singh · Anindita · Madhu

Abstract Thin films of pure Pd and composite of Pd and 1% multiwalled carbon nanotube have been obtained on glassy carbon electrodes by borohydride reduction method and investigated as electrocatalysts for the oxidation of phenol in acid medium at 25 °C, using cyclic voltammetry (CV), chronopotentiometry, and high-performance liquid chromatography. The CV study showed that both the electrocatalysts are quite stable and active for the phenol oxidation in acid medium. Further, these electrodes do not seem to undergo deactivation due to intermediates and products formed during the phenol oxidation. With the increase in phenol concentration from 2 to 25 mM, the peak current (I_p) increases initially, reaches maximum at about 15 mM, and tends to decrease thereafter. The peak potential (E_p) value was found to be practically unchanged with phenol concentration. The rate for phenol oxidation (I_p) at the surface of both the electrocatalysts increased with the decrease in pH of the reaction mixture. The electrocatalytic activity of the composite electrode was, however, higher than that of pure Pd under similar experimental conditions. Benzoquinone and hydroquinone were identified as the major phenol degradation intermediate products.

Keywords Phenol oxidation · Electrocatalysts · Composite films · Multiwalled carbon nanotubes

R. N. Singh (✉) · Anindita · Madhu
Chemistry Department, Science Faculty,
Banaras Hindu University,
Varanasi 221005, India
e-mail: rnsbhu@rediffmail.com

Introduction

Widespread contamination of water by phenol and its derivatives, particularly with chlorine, has been recognized as an issue of growing importance in recent years. Phenol is a known potential carcinogen and is of considerable health concern, even at low concentration [1]. The toxicity of chlorophenol increases with number of chloro-substituents but is lowered by the presence of chloro-substituent in the ortho position [2]. An increase in number of chloro-substituent can also promote the accumulation of such chemical compound in fish and other living organisms [3] and, thereby, increase their hazardous properties. It is reported that phenolic compounds concentrations above 2 mg l^{-1} are toxic to fish and that their concentrations between 10 and 100 mg l^{-1} result death in aquatic life within 96 h [4]. Several methods of treatments are known at present. Biological treatment, activated carbon adsorption, solvent extraction, chemical oxidation, and electrochemical methods are the most widely used methods for removing phenol and phenolic compounds from wastewater [5].

The transformation of toxic organic compounds into nontoxic ones using electrochemical methods has attracted wide attention during recent years [6–10] and recognized to be advantageous due to versatility, high efficiency, easy to control, amenability to automation, environment compatibility and cost effectiveness.

Electro-oxidation of most organic compounds, including phenol is possible theoretically in the potential region before oxygen evolution, but practically, oxidation reactions are sluggish, and their rates are limited more by kinetic than by thermodynamic factors [11]. It is, therefore, desired to search for low cost, efficient, and thermodynamically stable anodes so as to improve the oxidation kinetics.

A survey of literature reveals that the research work on the electrochemical detoxification/oxidation of organic pollutants seems to commence with the work of Comninellis [12] published in 1992. He studied the electrochemical oxidation of phenol at Pt and DSA anodes and demonstrated that traditional electrode materials (Pt, Ti/IrO_2, Ti/RuO_2, Ti/PbO_2) give relatively low current efficiency. Contrary to this, the SnO_2 anodes give high current efficiencies and also allow quasi complete total organic carbon elimination. The unexpected behavior of the SnO_2 anode has been ascribed to the change of chemical structure of the electrode surface during anodic polarization [13]. Subsequently, the electrochemical oxidation of benzoquinone on Ti/IrO_2 and Ti/SnO_2 in water [14] and on Fe-doped PbO_2 on Ti in 0.1 M H_2SO_4 [15] and 2-chlorophenol on a composite PbO_2/polypyrrole electrode in 0.1 M H_2SO_4 [16] have also been reported.

In recent years, the study on the electrochemical detoxification of organic pollutants, particularly phenol and its chloro-derivatives in wastewater, has become an important and burning research area of electrochemistry. In order to increase the efficiency vis-à-vis to reduce the cost of the process, a variety of electrode materials have been examined in the process of phenol oxidation. Some of the important electrode materials made of noble metals and based on metal oxides recently reported are Pt and Au [17–19], PbO_2 [20–23], SnO_2 [24–26], Ti/IrO_2, Ti/RuO_2, Ti/PbO_2, and Ti/SnO_2 [27], Bi/PbO_2 [28], Ti/SnO_2–PbO_2 [29], Ti/Sb–Sn–RuO_2–Gd, Ti/Sb–Sn–RuO_2 [10], RuO_2–TiO_2 [30], Bi-doped PbO_2 [31], Ti/TiO_2 doped with Ga^{3+} [32], Ti-based PbO2 with or without SnO_2 + Sb_2O_3 interlayers [33], Ti/RuO–Pt [34], V-doped MoO_x–C/Ti [35], Pt coated with quaternary metal oxide film containing Ti, Ru, Sn, and Sb oxides [36], mixed Ni–Mn oxides [37], mixed metal oxides SnO_2–RuO_2–IrO_2, Ta_2O_5–IrO_2, and RhO_2–IrO_2 immobilized on a Ti substrate using sol-gel technique [38], Ti/$RuO_{0.3}Pb_{(0.7-x)}TiO_4$ [39], nanostructured Pt–Fe/C [40]. A few other electrocatalysts such as synthetic diamond electrodes [6, 7, 41–44], boron-doped diamond films on tantalum [45], vitreous carbon [46], and carbon nanotubes [47] were also used as electrocatalysts for electrooxidation of phenols.

We have obtained thin films of Pd and Pd–1% multi-walled carbon nanotube (MWCNT) on glassy carbon (GC) electrodes through chemical reduction of $PdCl_2$ by $NaBH_4$ and investigated, for the first time, as electrocatalysts for oxidation of phenol in 0.5 M H_2SO_4. The use of MWCNT as support is based on its high surface area and the great number of mesopores which can lead to high metal dispersion and a good reactant flux in the tubular graphite structure. Besides, the metal–support interactions and the resistance of the support to oxidation are improved, while the metal sintering is disfavored [48]. Preliminary results of the investigation were very interesting as very negligible or

no inhibition effect of phenol oxidation intermediates/products was observed on Pd electrodes. Details of results are described in the present paper.

Experimental

Pd in powder form was obtained by dissolving required amount of $PdCl_2$ (anhydrous Merck) in 5 ml acidified double distilled water and subsequent reduction of metal ions by adding excess of $NaBH_4$ (Sigma-Aldrich, 98%) solution under stirred conditions as described elsewhere [49]. Similarly, 20 mg of Pd–1% MWCNT composite was prepared. For the purpose, MWCNTs (Aldrich, dia. + 110–170 nm, length=5–9 μm, Pr. No. 659258) were activated by refluxing in concentrated HNO_3 for 5 h as described elsewhere [50]. The required amount of activated MWCNTs was then added to a 5-ml acidified solution of $PdCl_2$ and stirred the solution well, and to this, an excess $NaBH_4$ solution was added under vigorous stirred condition to carry out the complete reduction of metal ions.

The catalyst obtained in powder form was mixed together with few milliliters of ethanol (Merck)–water mixture and then ultrasonicated for 15 min so as to obtain an ink. To obtain the electrode, two to three drops of ink were dropped onto a pretreated GC electrode through a syringe and dried, and then one drop of 1% Nafion solution (Alfa Aesar) was dropped over the dried catalyst layer to cover it. The catalyst electrodes, thus obtained, were finally irradiated with microwave (800 W) for 1 min. Prior to use as support for the catalyst, GC plates were first polished well on a microcloth pad on a polishing machine with alumina powder and then dipped in 0.2 M H_3PO_4 solution for 5 min, degreased with acetone by ultrasonication, washed with distilled water, and dried. Electrical contact with the catalyst over layer and electrode mounting were carried out as described elsewhere [51]. Physical characterization of the catalyst over layer on GC (geometrical surface area≈0.5 cm^2) has been carried out by XRD and SEM and already described in [49].

A conventional three-electrode single compartment Pyrex glass cell was used to carry out electrochemical studies. A Pt-foil (~8 cm^2) and a saturated calomel electrode were used as auxiliary and reference electrodes, respectively. All potentials reported in the text are with respect to this reference only. Cyclic voltammetry (CV) and chronopotentiometry studies were performed using an EG & G PAR model 273A galvanostat/potentiostat. The CV study was performed in the potential region, −0.20–1.30 V, in 0.5 M H_2SO_4 and in 0.5 M H_2SO_4 + x mM Phenol ($2 \leq x \leq 25$) at 25 °C. Prior to carry out the actual CV experiment, each electrode was cycled ten times at a scan rate of 50 mV s^{-1} in 0.5 M H_2SO_4. All electrochemical experi-
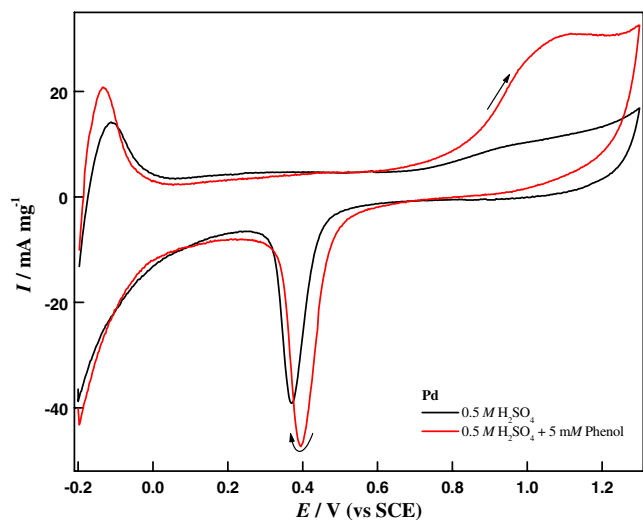
Fig. 1 Cyclic voltammogram of the Pd/GC electrode at 50 mV s^{-1} in 0.5 M H$_2$SO$_4$ and in 0.5 M H$_2$SO$_4$ + 5.0 mM phenol at 25 °C

ments were performed with triplicate electrodes in an Ar-deoxygenated electrolyte at 25 °C.

Analysis of oxidation intermediates/products

The oxidation products formed during the anodic oxidation of phenol were analyzed by high-performance liquid chromatography (HPLC) on a Younglin Acmc 9000, using a reversed phase column (Microsorb-MV 100-5 C18), UV detector (254 nm), and the mobile phase: 65% water–33% methanol (Merck: HPLC grade)–2% acetic acid (Qualigens: HPLC grade). Before each analysis, the sample and solvent were filtered.
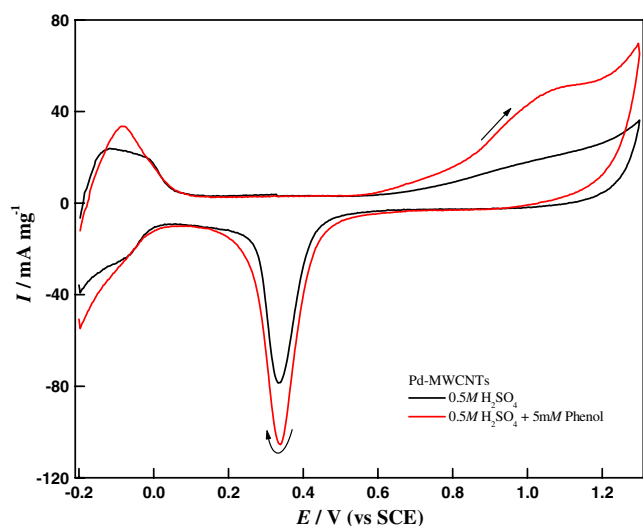

Fig. 2 Cyclic voltammogram of the Pd–1% MWCNT/GC electrode at 50 mV s^{-1} in 0.5 M H$_2$SO$_4$ and in 0.5 M H$_2$SO$_4$ + 5.0 mM phenol at 25 °C

Results and discussion

CV

CV of Pd/GC and Pd–1% MWCNT/GC electrodes in 0.5 M H$_2$SO$_4$ with and without phenol have been recorded at a scan rate of 50 mV s^{-1} between $E = -0.20$ and $E = 1.3$ V, and curves, so obtained, are reproduced in Figs. 1 and 2.

Features of curve shown in these figures appear to be more or less similar. In Figs. 1 and 2, cathodic and anodic curves produced in the potential region, −0.20 and 0 V, are due to the adsorption and desorption of hydrogen. The strong cathodic peak appeared at $E = 0.335$–0.40 V that corresponds to the reduction of palladium(II) oxide, formed due to transformation of Pd into palladium(II) oxide in the potential region 0.5–1.0 V under anodic conditions. At $E >$

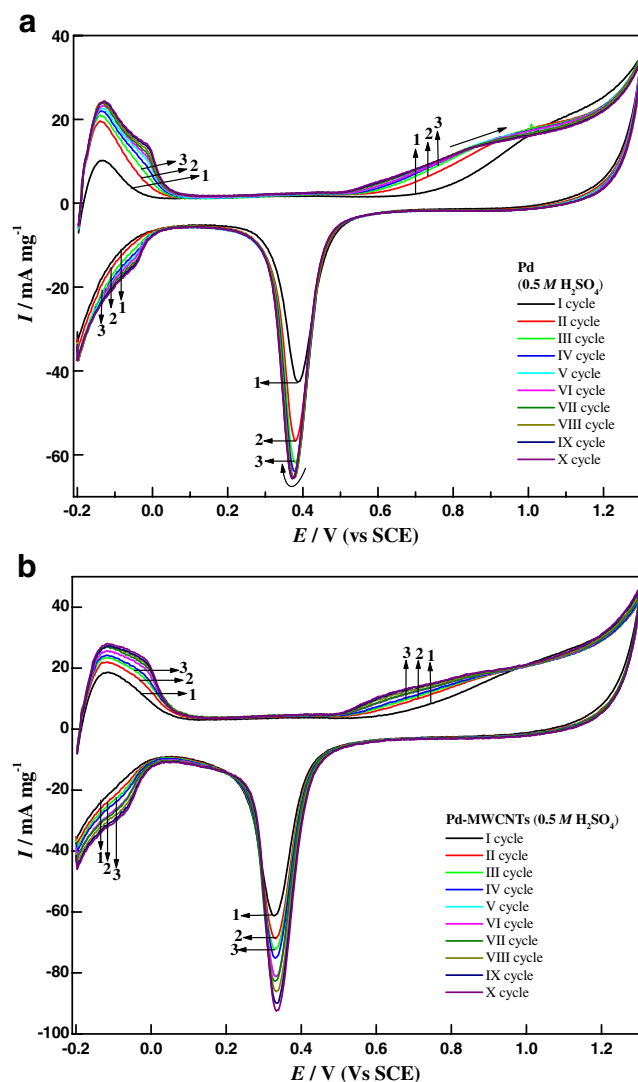Fig. 3 a Cyclic voltammogram of Pd/GC electrode at 50 mV s^{-1} in 0.5 M H$_2$SO$_4$ at varying scans. b Cyclic voltammogram of Pd–1% MWCNT/GC electrode at 50 mV s^{-1} in 0.5 M H$_2$SO$_4$ at varying scans
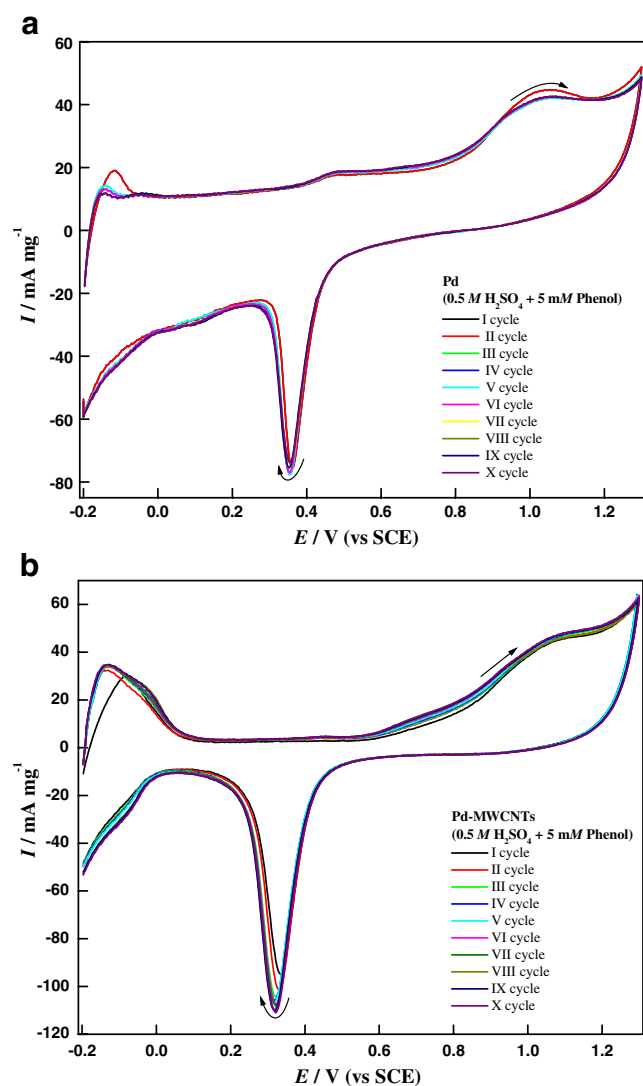
Fig. 4 **a** Cyclic voltammogram of Pd/GC electrode at 50 mV s^{-1} in 0.5 M H$_2$SO$_4$ + 5.0 mM Phenol at varying scans at 25 °C. **b** Cyclic voltammogram of Pd–1% MWCNT/GC electrode at 50 mV s^{-1} in 0.5 M H$_2$SO$_4$ + 5.0 mM phenol at varying scans at 25 °C

can be used to determine the electrochemical active surface area (EASA) of the catalyst electrode, using the relation, EASA=Q/Sl, where S is the proportionality constant used to relate charge with area and l is the catalyst loading in milligram. A charge value of 405 μC cm^{-2} is assumed for the reduction of palladium oxide monolayer [52]. To examine the stability, a set of ten consecutive cyclic runs at 50 mV s^{-1} were recorded on each electrode in 0.5 M H$_2$SO$_4$ and 0.5 M H$_2$SO$_4$ + 5.0 mM phenol at 25 °C. This experiment was carried out with triplicate electrodes. The total charge involved in the complete reduction of Pd(II) oxide into Pd metal in each cycle was determined by integrating the cathodic peak for the reduction of Pd(II) oxide. CV curves determined at varying scans on Pd/GC and Pd–1% MWCNT/GC in 0.5 M H$_2$SO$_4$ with and without 5 mM phenol are given in Figs. 3 and 4.

Figure 3a, b show that reproducible voltammetric responses are observed on both the electrodes only after three to four consecutive cycles. The EASA values of electrodes determined in 0.5 M H$_2$SO$_4$ were also found to be nearly constant, after the third cycle, regardless of the number of scans. Thus, the catalyst electrode seems to be quite stable in 0.5 M H$_2$SO$_4$ under potential cycling condition. The average values of EASA were found to be ~215 and ~366 cm^2 mg^{-1} in case of Pd/GC and Pd–1% MWCNT/GC electrodes, respectively. In estimation of average, all the values of EASA obtained after the third cycle were considered.

The observation of Fig. 3 further shows that, during consecutive cycles, there is a change in the feature of CV curves (i.e., curves slightly shift toward the higher current density side with increase in the cycle number) within the potential range corresponding to Pd(II)oxide formation, magnitude of change, however, being considerable in the first 3–4 cycles only. This can be caused due to slow diffusion of the electrolyte into the catalytic layer. As a result, some of the active Pd sites do not come in contact with the electrolyte. However, they become accessible to the electrolyte after 3–4 cycles, and reproducible voltammograms are obtained thereafter. This is also quite evident from the increase in the area under the cathodic peak for the palladium oxide reduction during the first 3–4 cycles.

Figure 4a, b represents the study of effect of number of cycles on the voltammogram of the electrodes in 0.5 M

1.25 V, the oxygen evolution reaction takes place. The comparison of Figs. 1 and 2 shows that oxidation of phenol takes place in the potential region which corresponds to the Pd(II) oxide formation.

As already reported [49], the total charge involved in the complete reduction of palladium oxide into Pd metal (Q)

Table 1 Effect of phenol concentration on the electrochemically active surface area of electrodes in 0.5 M H$_2$SO$_4$ at 50 mV s^{-1}

[Phenol] (mM)	0	2	5	10	15	20
Q (mC)	6.81 (14.53)	6.91 (15.15)	10.75 (16.23)	10.97 (16.11)	11.04 (16.20)	10.51 (14.99)
EASA (cm^2 mg^{-1})	~170 (~363)	~172 (~378)	~268 (~404)	~274 (~402)	~275 (~404)	~262 (~374)

Values shown with and without parentheses correspond to Pd–1% MWCNT and Pd electrodes, respectively
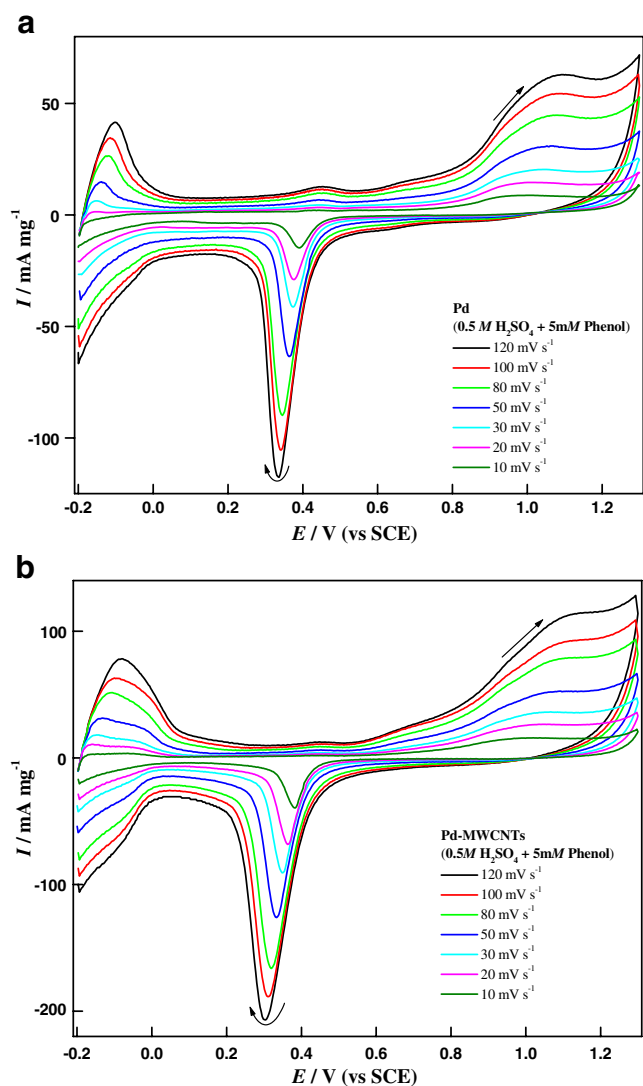
a

b

Fig. 5 a Cyclic voltammogram of Pd/GC electrode at varying scan rates in 0.5 M H_2SO_4 + 5.0 mM Phenol at 25 °C. **b** Cyclic voltammogram of Pd–1% MWCNT/GC electrode at varying scan rates in 0.5 M H_2SO_4 + 5.0 mM phenol at 25 °C

Fig. 6 Plot; I_p versus scan rate on the Pd/GC and Pd–1% MWCNT/GC electrodes in 0.5 M H_2SO_4 + 5 mM Phenol at 25 °C

intermediates/products. So, in subsequent studies, the oxidation peak current (I_p) of the first anodic cycle was considered for analysis of results.

The effect of phenol concentration on the EASA of electrocatalysts was also investigated, and results, so obtained, are shown in Table 1. This table shows that the EASA values for both the electrodes, Pd/GC and Pd–1% MWCNT, are practically constant regardless of concentration of phenol/intermediate oxidation products during cyclic run.

Effect of scan rate

The effect of scan rate has been observed on the cyclic voltammograms of the electrodes, Pd/GC and Pd–1%

H_2SO_4 + 5 mM phenol at the scan rate of 50 mV s^{-1}. Curves shown in Fig. 4 show that the phenol oxidation peak current (I_p) observed in the first cycle declines in the second cycle and it becomes more or less constant in the subsequent cycles (third to tenth). The observed decrease in the I_p values from first to second cycle was observed to be 2.5% to 8% with the use of Phenol concentration, 2 to 25 mM in the electrolyte (0.5 M H_2SO_4). However, the peak potential (E_p) value corresponding to the oxidation peak does not change with the number of cycle as well as phenol concentration. Thus, results show that both the electrocatalysts, Pd/GC and Pd–1% MWCNT, are quite stable during the oxidation of phenol in 0.5 M H_2SO_4. Small decrease in the peak current may be due to small coverage of the electrode surface by phenol or its oxidation
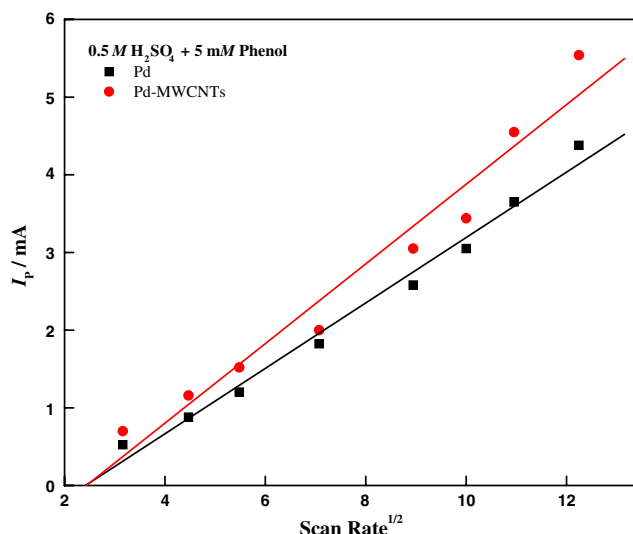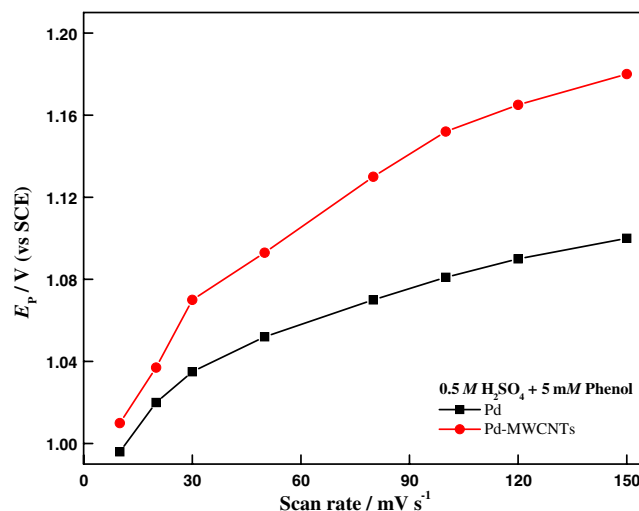

Fig. 7 Plot; E_p versus Scan rate on the Pd/GC and Pd–1% MWCNT/GC electrodes in 0.5 M H_2SO_4 + 5 mM phenol at 25 °C

MWCNT/GC, in the electrolyte solution, 0.5 M H_2SO_4 + 5 mM phenol, and the results, so obtained, are shown in Figs. 5a, b, 6, and 7.

Figure 6 demonstrates that in the case of both the electrodes, the I_p value increases linearly with the scan rate, suggesting that the oxidation of phenol at the Pd/GC and Pd–1% MWCNT electrodes is not a diffusion-controlled process but an adsorption-controlled one, under the applied experimental conditions [53]. Results shown in Fig. 6 displayed the following correlation between I_p and scan rate (v):

$$I_p = 0.51v - 1.25 \text{(for Pd} - 1\% \text{ MWCNT/GC electrode)} \tag{1}$$

$$I_p = 0.42v - 1.02 \text{(for Pd/GC electrode)} \tag{2}$$

With the increase in scan rate from 10 to 150 mV s^{-1}, the peak potential increased, showing constancy at higher scan rates (Fig. 7). The phenol oxidation peak current (I_p) corresponding to each scan rate was corrected for the background current measured at that scan rate.

Effect of phenol concentration

To investigate the effect of the phenol concentration on the rate of electrochemical oxidation, the CV of the Pd/GC and Pd–1% MWCNT/GC electrodes has been recorded at 50 mV s^{-1} in 0.5 M H_2SO_4 containing varying concentrations of phenol from 2 mM to 25 mM, and results, so obtained, are shown in Fig. 8. This figure shows that with the increase in phenol concentration from
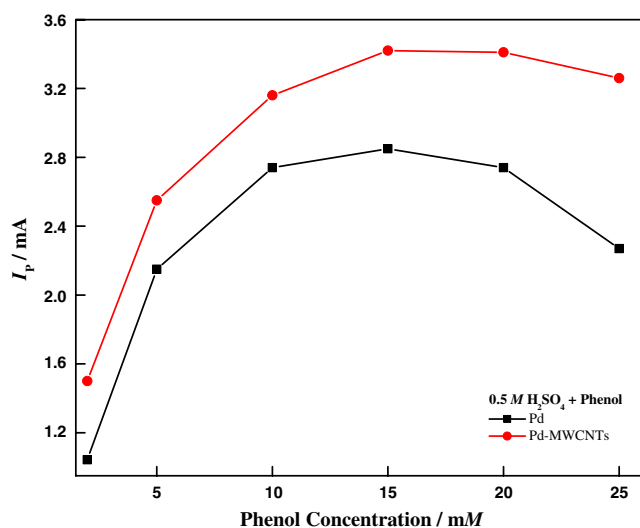
Fig. 9 Effect of pH on rate of phenol oxidation (I_p) at the Pd/GC and Pd–1% MWCNT/GC electrodes in H_2SO_4 + 5 mM Phenol at 25 °C; scan rate=50 mV s^{-1}

2 to 25 mM, the I_p value initially increases and attains a maximum at about 15 mM and tends to decrease thereafter. A more or less similar complex dependence of the peak current on the phenol concentration has also been found on Pt electrode in 0.5 M H_2SO_4 [54]. On the other hand, the E_p value is found to be practically unchanged with the phenol concentration. The observed decrease in the oxidation peak current at the higher phenol concentrations is not very clear. However, it is considered that phenol, at higher concentrations, forms larger amounts of phenoxy radicals which can result to the formation of polymeric compounds, and consequently, the electrode gets deactivated.

Fig. 8 Effect of phenol concentration on the rate of phenol oxidation at the Pd and Pd–1% MWCNT/GC electrodes in 0.5 M H_2SO_4 at 25 °C; scan rate=50 mV s^{-1}
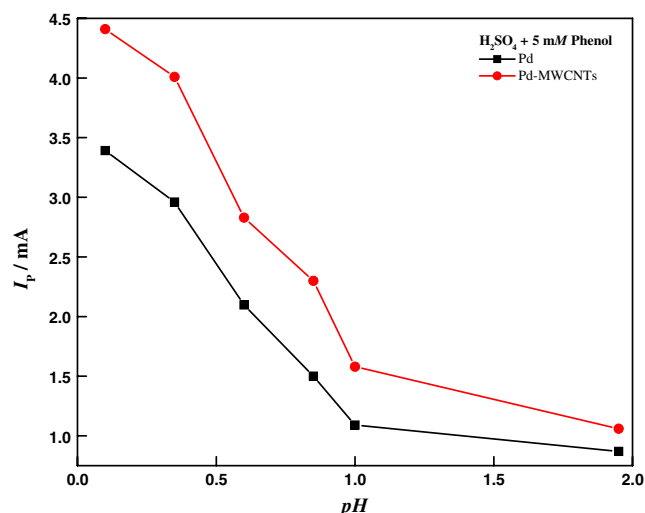
Table 2 Results of analyses of the reaction mixture at different electrolysis times

Electrolysis time (min)	Analysis products (ppm)			
	Phenol	Benzoquinone	Hydroquinone	Catechol
0	496.4	–	–	–
30	495.3	0.5	0.7	–
60	491.6	0.8	1.1	0.1
90	489.2	1.1	1.9	0.1
120	488.4	2.4	2.7	0.2
180	481.6	1.0	4.0	0.2
240	479.5	0.7	4.3	0.2
300	477.0	0.6	4.7	0.3

Geometrical area of the electrode=1 cm^2, duration of electrolysis=5 h, [H_2SO_4]=0.5 M, j=10 mA cm^{-2}, [Phenol]=500 ppm, Temp=25 °C

Effect of pH

The study of effect of pH has been carried out on the phenol oxidation current density keeping the phenol concentration (5 mM) in the electrolyte constant. For the purpose, different concentrations of H_2SO_4 solutions, each containing 5 mM phenol, were prepared and used in the study. The pH of each solution containing phenol was measured using a pH meter. Results of the investigation are shown in Fig. 9. This figure demonstrates that the I_p value grows almost linearly with the decrease in pH of the solution from pH 1 to 0.1. At pH>1, the I_p value decreases gradually with pH, indicating constancy.

Product analysis

For identification of phenol oxidation products, the chronopotentiometry study of the electrocatalysts has been carried out at a constant current density of 10 mA cm^{-2} in 0.5 M H_2SO_4 + 500 ppm phenol at 25 °C. The quantitative analyses of phenol and its oxidation products were determined by HPLC. Samples were taken at appropriate time intervals and immediately analyzed. The separation was performed using a reversed phase column and flow rate of 1.0 ml min^{-1}.

Chromatography results indicate that the major intermediate products formed during the electrooxidation of phenol are hydroquinone and benzoquinone; catechol is formed as a minor product. The subsequent oxidation products for these intermediates could not be detected by HPLC. Results of HPLC analyses are given in Table 2. This table shows that with the passage of electrolysis time, the amount of benzoquinone initially increases, reaches maximum, and decreases thereafter; in contrast, the amount of hydroquinone gradually increases showing constancy. On the other hand, during the electrolysis, the formation of catechol is small and seems to be nearly constant.

Chronopotentiometry of the electrocatalyst carried out at a current density of 10 mA cm^{-2} in 0.5 M H_2SO_4 containing 5 mM hydroquinone indicated the formation of oxalic acid as the reaction product, but similar test performed with oxalic acid did not indicate its oxidation further. So, it can be said that the end product of the phenol oxidation at Pd electrodes is oxalic acid.

Conclusions

The study indicates that Pd/GC and Pd–1% MWCNT electrodes are quite stable and do not undergo deactivation by the phenol oxidation intermediates and products under the employed experimental conditions (phenol concentration<10 mM). Thus, the results show that Pd electrode with improved electrocatalytic properties by suitable means can be a potential anode for detoxification of phenol. The electrocatalytic activity of the composite electrode was greater than the Pd/GC electrode. The rate of phenol oxidation increased with decrease in pH of the reaction mixture. The investigation of mechanism is continued.

References

1. Idris A, Saed K (2002) Global Nest: the Int J 4:139
2. Martin TM, Young DM (2001) Chem Res Toxicol 14:1378
3. Kishino T, Kobayshi K (1996) Water Res 30:393
4. Zhang H, Sorial GA (2005) Electrochemical process for oxidative destruction of 4-chlorophenol. Presented at AIChE 2005 Annual Meeting, Cincinnati, OH, October 30–November 4, 2005
5. Skowronski JM, Krawczyk P (2007) J Solid state Electrochem 11:223
6. Rodgers JD, Jedral W, Bunce NJ (1999) Environ Sci Technol 33:1453
7. Fryda M, Dietz A, Herrmann D, Hampel A, Schafer L, Klages CP, Perret A, Haenni W, Comninellis Ch, Gandini D (2000) Book of abstracts of 51th Annual ISE Meetings, p 598, Warsaw University.
8. Li XY, Cui YH, Feng YJ, Xie ZM, Gu JD (2005) Water Res 39:1972
9. Iniesta J, Michaud PA, Panizza M, Cerisola G, Aldaz A, Comninellis Ch (2001) Electrochim Acta 46:3573
10. Feng YJ, Li XY (2003) Water Res 37:2399
11. Comninellis Ch (1994) Electrochim Acta 39:1857
12. Comninellis Ch (1992) Process Protection 70:219
13. Comninellis Ch, Pulgarin C (1993) J Appl Electrochem 23:108
14. Pulgarin C, Adler N, Peringer P, Comninellis Ch (1994) Water Res 28:887
15. Feng J, Houk LL, Johnson DC, Lowery SN, Carey JJ (1995) J Electrochem Soc 142:3626
16. Hwang BJ, Lee KL (1996) J Appl Electrochem 26:153
17. Lapuente R, Cases F, Garces P, Morallon E, Vazquez JL (1998) J Electroanal Chem 451:163
18. Ezerskis Z, Jusys Z (2002) J Appl Electrochem 32:755
19. Andreescu S, Andreescu D, Sadik OA (2003) Electrochem Commun 5:681
20. Houk LL, Johnson SK, Feng J, Houk RS, Johnson DC (1998) J Appl Electrochem 28:1167
21. Tahar NB, Savall A (1998) J Electrochem Soc 145:3427
22. Tahar NB, Savall A (1999) J Appl Electrochem 29:277
23. Fleszar B, Ploszynska J (1985) Electrochim Acta 30:31
24. Kotz R, Stucki S, Carcer B (1991) J Appl Electrochem 21:14
25. Stucki S, Kotz R, Carcer B, Suter W (1991) J Appl Electrochem 21:99
26. Comninellis Ch, Pulgarin C (1991) J Appl Electrochem 21:703
27. Comninellis Ch, Nerini A (1995) J Appl Electrochem 25:23
28. Kawagoe KT, Johnson DC (1994) J Electrochem Soc 141:3404
29. Gherardini L, Comninellis Ch, Vatistas N (2001) Ann Chem 91:161
30. Panic VV, Dekanski AB, Vidakovic TR, Miskovic-Spankovic VB, Javanovic BZ, Nikolic BJ (2004) J Solid State Electrochem 9:43
31. Borras C, Laredo T, Mostany J, Scharifker BR (2004) Electrochim Acta 49:641

32. Andrade LS, Laurindo EA, de Oliveira RV, Rocha-Filho RC, Cass QB (2006) J Braz Chem Soc 17:369
33. Wang Y, Gu B, Xu W, Lu L (2007) Xiyou Jinshu Cailiao Yu Gongcheng 36:874
34. Li M, Feng C-P, Hu W-W, Zhang Y-Y, Sugiura N (2008) Huanjing Kexue Yu Jishu 31:84
35. Liu Q, Liu H-Y (2008) Xinyang Shifan Xueyuan Xuebao, Ziran Kexueban 21:57
36. Johnson SK, Houk LL, Feng J, Houk RS, Johnson DC (1999) Environ Sci Technol 33:2638
37. Stoyanova M, Christoskova St, Georgieva M (2003) Appl Catal A Gen 249:295
38. Makgae ME, Klink MJ, Crouch AM (2008) Appl Catal B: Environ 84:659
39. Cestarolli DT, de Andrade AR (2007) J Electrochem Soc 154:E25
40. Li W, Zhou W, Li H, Zhou Z, Zhou B, Sun G, Xin Q (2004) Electrochim Acta 49:1045
41. Comninellis Ch, Duo I, Michaud PA (2000) Book of abstracts of 8th international Fisher symposium on electrochemistry and environment, pp 49–52, Universitat Karlsruhe
42. Gherardini L, Michaud PA, Panizza M, Comninellis Ch, Vatistas N (2001) J Electrochem Soc 148:D78
43. Hagans PL, Natishan PM, Stoner BR, O'Grady WE (2001) J Electrochem Soc 148:E298
44. Rodrigo MA, Michaud PA, Duo I, Panizza M, Cerisola G, Comninellis Ch (2001) J Electrochem Soc 148:D60
45. Chang M, Gao C (2009) Huagong Xinxing Cailiao 37:37
46. Belhadj Tahar N, Savall A (2009) Electrochim Acta 55:465
47. Peng J, Mu Q-W, Zhang C (2006) Chongqing Daxue Xuebao, Ziran Kexueban 29:135
48. Bianchini C, Shen PK (2009) Chem Rev 109:4143
49. Singh RN, Singh A, Anindita (2009) Carbon 47:271
50. Wang J, Xi J, Bai Y, Shen Y, Sun J, Chen L et al (2007) J Power Sources 164:555
51. Singh RN, Sharma T, Singh A, Anindita, Mishra D, Tiwari SK (2008) Electrochim Acta 53:2322
52. Singh RN, Singh A, Anindita (2009) Int J Hydrogen Energy 34:2052
53. Li C (2007) Microchim Acta 157:21
54. Arslan G, Yazici B, Erbil M (2005) J Hazardous Mater 124:37